International Journal of Trend in Scientific Research and Development (IJTSRD)
Volume 6 Issue 7, November-December 2022 Available Online: www.ijtsrd.com e-ISSN: 2456 – 6470

Solving Fractional Type of Astronomy Equation by Fractional Order of Rationalized Haar Operational Matrices

Ali Pirkhedri

Department of Computer Engineering, Islamic Azad University, Marivan Branch, Kurdistan, Iran

ABSTRACT

Numerical solution of fractional Lane-Emden equation which is the nonlinear singular initial value problem in astrophysics has been proposed by fractional order of Rationalized Haar operational matrices based on collocation method. The advantage of our technique is that the computational speed is high due to using the RH operational matrices and the convergence rate is exponential. We investigate two examples to test the accuracy, speed and efficiency of this new method in which these evaluations confirmed our claim.

KEYWORDS: *Rationalized Haar; Operational Matrix; Collocation; Fractional Order; Lane-Emden; Exponential Convergence;*

How to cite this paper: Ali Pirkhedri "Solving Fractional Type of Astronomy Equation by Fractional Order of Rationalized Haar Operational Matrices" Published in International Journal of Trend in Scientific Research and Development (ijtsrd), ISSN: 2456-6470, Volume-6 | Issue-7, December 2022, pp.696-703, URL: www.ijtsrd.com/papers/ijtsrd52389.pdf

IJTSRD52389

INTRODUCTION

Fractional differential equations are generalizations of classical differential equations, which are obtained by replacing integer-order derivatives by fractional ones. Their advantages comparing with integer-order partial differential equations are the capability of simulating natural physical process and dynamic system more accurately. Furthermore, the fractional order models of real systems are regularly more adequate than usually used integer order models [1].

The ordinary Lane-Emden equation describes the temperature variation of a spherical gas cloud under the mutual attraction of its molecules and published by Lane [2] and further explored in detail by Emden [3].

Lane-Emden equation is a second-order ordinary differential equation with an arbitrary index, known as the polytropic index, that deals with the issue of energy transport, through the transfer of material between different levels of the star [4].

The ordinary Lane-Emden does not describe the dynamics of systems in complex media accurately. Also, the memory effects are better described within the fractional derivatives, therefore the fractional Lane-Emden equations extract hidden aspects of the complex phenomena and it can describe the parameters better and more accurately [5].

In this paper, we study the Caputo fractional derivative of Lane-Emden type equation as [6]:

$$D_t^{\alpha} y(t) + \frac{\lambda}{t^{\alpha-\beta}} D_t^{\beta} y(t) + f(t,y) = g(t), \qquad 0 < t < b, \quad \lambda \geq 0, \tag{1}$$

with initial conditions

$$y(0) = A, \quad y'(0) = B, \tag{2}$$

where $0 < \alpha \leq 2, 0 < \beta \leq 1$ and $D_t^{\alpha}, D_t^{\beta}$ refer to the Caputo fractional derivative of order α, β with respect to t, and parameters A, B and λ is constant, $f(t,y)$ is a nonlinear function of t, y and $g(t)$ is a continuous real valued function in $C[0,b)$.

The single standard and general solution algorithm for problems regarding fractional calculus has not yet been constituted and finding affirmative, accurate, stable and credible solution methods along with fast time computation order is beneficial.

For the solution of nonlinear and singular fractional Lane-Emden equations which are difficult to solve there are many numerical and analytical methods such as, differential transform method [6], collocation technique [7], finite difference algorithm[8], Homotopy analysis approximation [9], reproducing kernel method [10], hybrid wavelet method [11], Legendre wavelets spectral technique [12], coupling of wavelets and Laplace transform [13], spectral Legendre's derivative algorithms [14], discontinuous finite element approximation [15] and Galerkin operational matrices [16].

In this paper, RH collocation method based on fractional order of operational matrices is developed to obtain solutions of singular fractional Lane–Emden type equations. The properties of the RH orthogonal functions are used to convert the problem into a system of algebraic equations which can be solved by suitable algorithms with exponential convergence rate.

The organization of the rest of this paper is as follows: In Section 2, we describe a short introduction to the basic definitions of the fractional calculus and Rationalized Haar properties which drive some tools for developing our method. In Section 3, we summarize the application of the RH operational matrices collocation method for solving the model equation. In Section 4, the proposed method is applied to some types of fractional Lane-Emden equations, and comparisons are made with the existing analytic solutions that were reported in other published works in the literature. The conclusions are described in the final section.

Basic definitions

A. Definitions of fractional derivatives and integrals

In this section, we start with recalling the essentials of the fractional calculus [1].

Definition 1. For m to be the smallest integer that exceeds α, Caputo's time-fractional derivative operator of order $\alpha > 0$ is defined as:

$$ {}_a^C D_t^\alpha y(t) = \begin{cases} I_t^{m-\alpha} D_t^m y(t), & m-1<\alpha<m, \\ D_t^m y(t), & \alpha = m, m \in N, \end{cases} \quad (3)$$

where

$$I_t^\alpha y(t) = \frac{1}{\Gamma(\alpha)} \int_0^t (t-\tau)^{\alpha-1} y(\tau) d\tau, \quad t,\alpha > 0, \quad (4)$$

Some of the most important properties of operator I_t^α, D_t^α is as follows:

$$\begin{aligned} I_t^\alpha(t^\mu) &= \frac{\Gamma(\mu+1)}{\Gamma(\mu+\alpha+1)} t^{\mu+\alpha}, \\ I_t^\alpha(x^\gamma t^\mu) &= x^\gamma I_t^\alpha(t^\mu), \\ D_t^\alpha(t^\mu) &= \frac{\Gamma(\mu+1)}{\Gamma(\mu-\alpha+1)} t^{\mu-\alpha}, \end{aligned} \quad (5)$$

$$D_t^\alpha(\kappa y(t) + \rho s(t)) = \kappa D_t^\alpha y(t) + \rho D_t^\alpha s(t),$$

where κ and ρ are constants.

B. Rationalized Haar functions

The orthogonal set of RH functions is a group of square waves with magnitude of ± 1 in some intervals and zeros elsewhere [17]. The RH functions is defined on the interval $C = [0, b)$ by:

$$h_u(t) = \begin{cases} -1, l_1 \le t < l_{\frac{1}{2}} \\ 1, l_{\frac{1}{2}} \le t < l_0 \\ 0, otherwise \end{cases}, (6)$$

where

$$l_q = \frac{n-q}{2^m} b, \quad q = 0, \frac{1}{2}, 1. (7)$$

The value of u is defined by two parameters m and n as:

$$u = 2^m + n - 1, \quad m = 0,1,2,\dots, \quad n = 1,2,3,\dots,2^m. (8)$$

$h_0(t)$ is defined for $m = n = 0$ and is given by:

$$h_0(t) = 0, \quad 0 \le t < b. (9)$$

We can expand any function $y(t) \in L^2[0,b)$ in first k terms of RH functions as:

$$y(t) \simeq \sum_{u=0}^{k-1} x_u h_u(t) = X^T \phi_k(t), (10)$$

where

$$k = 2^{s+1}, s = 0,1,2, \dots$$

The RH functions coefficient vector X and RH functions vector $\phi_k(t)$ are defined as:

$$X = [x_0, \quad x_1, \quad \dots, \quad x_{k-1}]^T, (11)$$

$$\phi_k(t) = [h_0(t), \quad h_1(t), \quad \dots, \quad h_{k-1}(t)]^T, (12)$$

The matrix $\Phi_{k\times k}$ can be expressed as:

$$\Phi_{k\times k} = \left[\phi_k\left(\frac{1}{2k}\right), \phi_k\left(\frac{3}{2k}\right), \dots, \phi_k\left(\frac{2k-1}{2k}\right)\right]. (13)$$

C. Rationalized Haar operational matrices of fractional order integration

The integration of the $\phi_k(t)$ defined in Eq. (12) is given by:

$$\int_0^t \phi_k(s) ds \simeq J\phi_k(t), (14)$$

where $J = J_{k\times k}$ is the $k \times k$ operational matrix for integration and is given in [18] as:

$$J_{k\times k}=\frac{b}{2k}\begin{bmatrix} 2kJ_{\left(\frac{k}{2}\right)\times\left(\frac{k}{2}\right)} & -\Phi_{\left(\frac{k}{2}\right)\times\left(\frac{k}{2}\right)} \\ \Phi^{-1}_{\left(\frac{k}{2}\right)\times\left(\frac{k}{2}\right)} & 0 \end{bmatrix}, (15)$$

where $\Phi_1=[1]$, $J_1=\left[\frac{1}{2}\right]$.

Also, we obtain the Rationalized Haar operational matrix of the fractional order integration $(I_t^\alpha\phi_k)(t)$ [19] as:

$$(I_t^\alpha\phi_k)(t)=J_{k\times k}^\alpha\phi_k(t), (16)$$

where

$$J_{k\times k}^\alpha=\Phi_{k\times k}F^\alpha\Phi_{k\times k}^{-1}, (17)$$

where

$$F^\alpha=\frac{1}{k^\alpha}\frac{1}{\Gamma(\alpha+2)}\begin{bmatrix} 1 & \omega_1 & \omega_2 & \dots & \omega_{k-1} \\ 0 & 1 & \omega_1 & \dots & \omega_{k-2} \\ 0 & 0 & 1 & \dots & \omega_{k-3} \\ 0 & 0 & 0 & \ddots & \vdots \\ 0 & 0 & 0 & 0 & 1 \end{bmatrix}, (18)$$

With $\omega_r=(r+1)^{\alpha+1}-2r^{\alpha+1}+(r-1)^{\alpha+1}$.

Theorem. 1 Assume that $y^{(p)}(t)$ is continuous and bounded on $(0,1)$, then there is [20] :

$$\exists D>0,\quad \forall t\in(0,1)\quad \left|y^{(p)}(t)\right|\le D. (19)$$

Then, the error norm at Tth level of resolution satisfies the following inequality:

$$\parallel D_\star^\alpha y(t)-D_\star^\alpha y_T(t)\parallel_E\le \frac{1}{T^{p-\alpha}}\frac{D}{\Gamma(p-\alpha).(p-\alpha)}\frac{1}{\sqrt{1-2^{2(\alpha-p)}}}, (20)$$

where $D_\star^\alpha y_T(t)$ is the following approximation of $D_\star^\alpha y(t)$,

$$D_\star^\alpha y_T(t)=\sum_{u=0}^{T-1}x_u\,h_u(t), (21)$$

and

$$\parallel y(t)\parallel_E=\left(\int_0^1 y^2(t)dt\right)^{\frac{1}{2}}. (22)$$

Implementation of Rationalize Haar operational matrices for solving the model

To solve Eq. (1) with boundary conditions in Eq. (2) we let:

$$y''(t)=\sum_{u=0}^{k-1}x_u\,h_u(t)=X^T\phi_k(t), (23)$$

where

$$u=2^m+n-1,\quad m=0,1,2,\dots,\quad n=1,2,3,\dots,2^m. (24)$$

Using Eqs. (14) and (23) we get:

$$y'(t)=X^TJ\phi_k(t)+B, (25)$$

and

$$y(t)=X^TJ\int_0^t\phi_k(\ell)d\ell+Bt+A=X^TJ^2\phi_k(t)+Bt+A. (26)$$

Also by using Eq.(5), for $1<\alpha\le 2, 0<\beta\le 1$, we have $D_t^\alpha t=0, D_t^\beta t=\frac{t^{1-\beta}}{\Gamma(2-\beta)}, D_t^\alpha A=D_t^\beta A=0$, and using Eqs.(26), (3) we have:

$$D_t^\alpha y(t)=X^TJ^{(2-\alpha)}\phi_k(t)+BD_t^\alpha t+D_t^\alpha A=X^TJ^{(2-\alpha)}\phi_k(t), (27)$$

$$D_t^\beta y(t)=X^TJ^{(2-\beta)}\phi_k(t)+BD_t^\beta t+D_t^\beta A=X^TJ^{(2-\beta)}\phi_k(t)+\frac{Bt^{1-\beta}}{\Gamma(2-\beta)}. (28)$$

Using Eqs. (1), (27) and (28) we get:

$$X^TJ^{(2-\alpha)}\phi_k(t)+\frac{\lambda}{t^{\alpha-\beta}}\left(X^TJ^{(2-\beta)}\phi_k(t)+\frac{Bt^{1-\beta}}{\Gamma(2-\beta)}\right)+f(t,X^TJ^2\phi_k(t)+Bt+A)=g(t). (29)$$

The residual $Res_k(t)$ for Eq. (1) can be written as:

$$Res_k(t)=X^TJ^{(2-\alpha)}\phi_k(t)+\frac{\lambda}{t^{\alpha-\beta}}\left(X^TJ^{(2-\beta)}\phi_k(t)+\frac{Bt^{1-\beta}}{\Gamma(2-\beta)}\right)+f(t,X^TJ^2\phi_k(t)+Bt+A)-g(t). (30)$$

The equations for obtaining the coefficients x_u arises from equalizing $Res_k(t)$ to zero at k RH collocation points defined by:

$$t_i=\frac{2i-1}{2k}b,\quad i=1,2,\dots,k. (31)$$

By substitution collocation points $t_i, i=1,2,\dots,k$ in $Res_k(t)$ and equalizing to zero we have:

$$Res_k(t_i)=0,\quad i=1,2,\dots,k. (32)$$

Eq. (32) gives k nonlinear algebraic equations which can be solved for the unknown coefficients $x_u, u=0,1,\dots,k-1$ by using the well-known Newton's method. Consequently, $y(t)$ given in Eq. (1) can be calculated.

Numerical results and illustrative examples

In this section, we solve the model numerically by the proposed method and show the efficiency of the method with the numerical results of two examples.

Example 1. We consider the following fractional equation which has been solved in [6],[7]:

$$D_t^\alpha y(t)+\frac{\lambda}{t^{\alpha-\beta}}D_t^\alpha y(t)+\frac{1}{t^{\alpha-2}}y(t)=s(t), (33)$$

with initial conditions

$$y(0)=0,\quad y'(0)=0, (34)$$

where $s(t)=t^{2-\alpha}\left(6t\left(\frac{t^2}{6}+\frac{\Gamma(4-\beta)+\lambda\Gamma(4-\alpha)}{\Gamma(4-\beta)\Gamma(4-\alpha)}\right)-2\left(\frac{t^2}{2}+\frac{\Gamma(3-\beta)+\lambda\Gamma(3-\alpha)}{\Gamma(3-\beta)\Gamma(3-\alpha)}\right)\right)$.

The exact solution to this problem for $\alpha=1.5, \beta=0.5$ and $\lambda=1$ is t^3-t^2.

Table 1 shows the comparison of the $y(t)$ between numerical solutions obtained by the method proposed in this letter for $k = 8,16,32,64$ and their absolute errors with respect to the exact solution. Fig. 1. shows the numerical and analytic graph of solution of Eq.(33) for $k = 32$. The graph of absolute errors for $k = 32$ at RH collocation points $t_i = \frac{2i-1}{2k}, i = 1,2,\ldots,k$ is shown in Fig. 2.

Example 2. Consider to the following equation [6], [7]:

$$D_t^{\alpha} y(t) + \frac{\lambda}{t^{\alpha-\beta}} D_t^{\alpha} y(t) + \frac{1}{t^{\alpha-2}} y(t) = r(t), (35)$$

with initial conditions

$$y(0) = 0, \quad y'(0) = 0, (36)$$

where $r(t) = t^{2-\alpha}\left(2\left(\frac{t^2}{2} + \frac{\Gamma(3-\beta)+\lambda\Gamma(3-\alpha)}{\Gamma(3-\beta)\Gamma(3-\alpha)}\right) - 6t\left(\frac{t^2}{6} + \frac{\Gamma(4-\beta)+\lambda\Gamma(4-\alpha)}{\Gamma(4-\beta)\Gamma(4-\alpha)}\right)\right)$. The exact solution to this problem for $\alpha = 1.5, \beta = 1$ and $\lambda = 1$ is $t^2 - t^3$.

In table 2, we report the absolute errors with respect to the exact solution for different values k. In Fig. 3, the graph of $y(t)$ for $k = 32$ and exact solution is plotted.

The $L^2 - Error$ and $L^{\infty} - Error$ are used to explore the dependence of errors on the parameters k. Fig. 4 displays the logarithmic scale of error versus k for $k = 4,8,16,32,64,128$ at RH collocation points. Since in this semi-log representation the error variations are approximately linear versus k, we observe that the values of error decay exponentially.

Example 3. Consider to the following equation [21]:

$$D_t^{2\alpha} y(t) + \frac{2\alpha}{t^{\alpha}} D_t^{\alpha} y(t) + 1 = 0, 0 < \alpha \leq 1, (37)$$

with initial conditions

$$y(0) = 1, \quad y'(0) = 0. (38)$$

The exact solution to this problem is $1 - \frac{t^{2\alpha}}{6\alpha^2}$. Table 3 displays the max absolute errors with respect to the exact solution for different values of k, α at RH collocation points. We can see clearly that better accuracy can be achieved by increasing the values of k and the values of error decrease when the values of α converge to 1. Fig. 5 shows the approximate solution obtained by present method for $k = 64$ for different values of α.

Example 4. Consider to the following equation [21]:

$$D_t^{2\alpha} y(t) + \frac{2\alpha}{t^{\alpha}} D_t^{\alpha} y(t) + e^{y}(t) = 0, 0 < \alpha \leq 1, (39)$$

with initial conditions

$$y(0) = 1, \quad y'(0) = 0. (40)$$

The exact solution to this problem is $-\frac{t^{2\alpha}}{6\alpha^2} + \frac{t^{4\alpha}}{120\alpha^4} - \frac{t^{6\alpha}}{1890\alpha^6}$.

Fig. 6 displays the behavior of the solution at $\alpha = 0.5, 0.75, 0.85, 1$ for $k = 64$. Fig. 7 displays the logarithmic scale of error versus k for $k = 8,16,32,64$ at RH collocation points.

Conclusion

RH operational matrices have been successfully employed to obtain accurate numerical solutions of fractional Lane–Emden type equations with linear and nonlinear terms, with fast convergence rate. The comparison between numerical and analytic methods has been made and it can be clearly seen from absolute errors in tables 1,2 and 3 that the numerical results of the suggested method converges to the exact solution by increasing the values of k. In addition, the properties of the RH functions have been used to convert the problem into a system of algebraic equations which can be conveniently solved by suitable algorithms.

Table 1 Absolute errors with respect to the exact solution for $k = 8, 16, 32, 64$ for Example 1

$k \backslash t$	0.2	0.4	0.6	0.8	1
8	1.165e-3	1.863e-3	1.793e-3	1.539e-3	1.161e-3
16	2.105e-4	2.256e-4	2.098e-4	1.759e-4	1.303e-4
32	1.017e-6	1.377e-6	1.437e-6	1.292e-6	1.004e-6
64	1.872e-8	1.997e-8	1.840e-8	1.526e-8	1.118e-8

Table 2. Absolute errors with respect to the exact solution for $k = 8, 16, 32, 64$ for Example 2.

$k \backslash t$	0.2	0.4	0.6	0.8	1
8	1.719e-3	1.924e-3	1.840e-3	1.572e-3	1.182e-3
16	2.174e-4	2.317e-4	2.145e-4	1.794e-4	1.326e-4
32	1.110e-6	1.443e-6	1.483e-6	1.324e-6	1.024e-6
64	1.922e-8	2.038e-8	1.869e-8	1.547e-8	1.131e-8

Table 3. Max absolute errors with respect to the exact solution for $k = 8, 16, 32, 64$ for different values of α at RH collocation points for Example 3.

k \ α	0.25	0.5	0.75	0.85	1
8	2.004e-3	1.735e-3	1.254e-3	1.193e-3	1.126e-3
16	4.019e-4	3.758e-4	3.024e-4	1.994e-4	1.728e-4
32	3.128e-6	2.854e-6	2.019e-6	1.917e-6	1.520e-6
64	2.954e-8	2.158e-8	1.978e-8	1.287e-8	1.015e-8

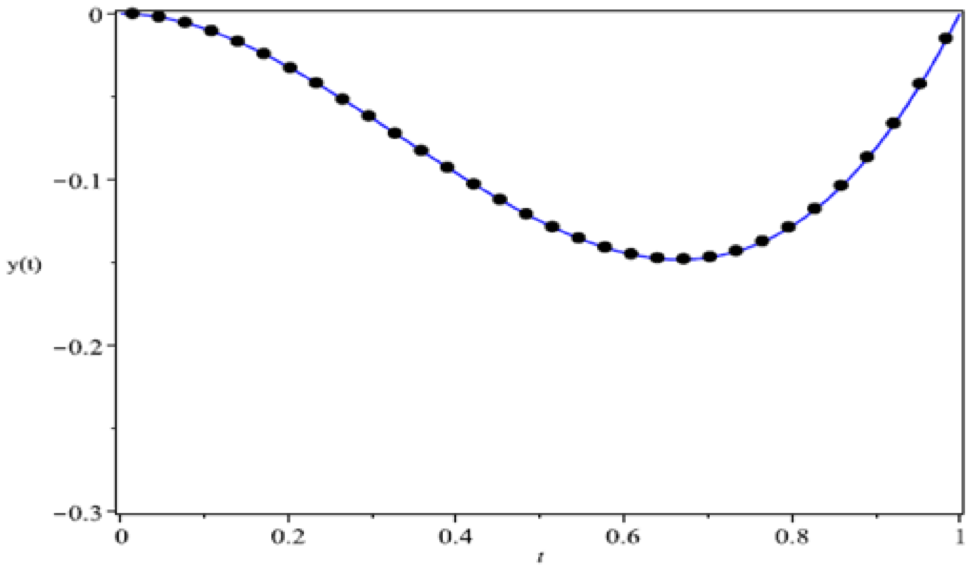

Fig. 1. Numerical (solid circle) and analytic (solid line) graph of solution of Example. 1, for $k = 32$.

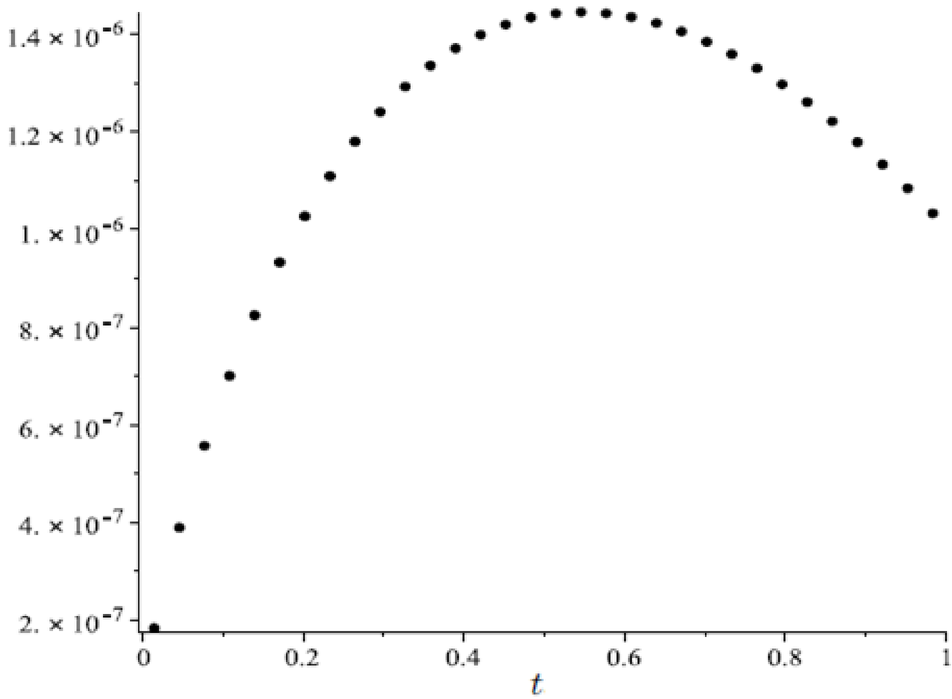

Fig. 2. Absolute errors at RH collocation points $t_i = \frac{2i-1}{2k}, i = 1, 2, \ldots, k$, for Example. 1, for $k = 32$.

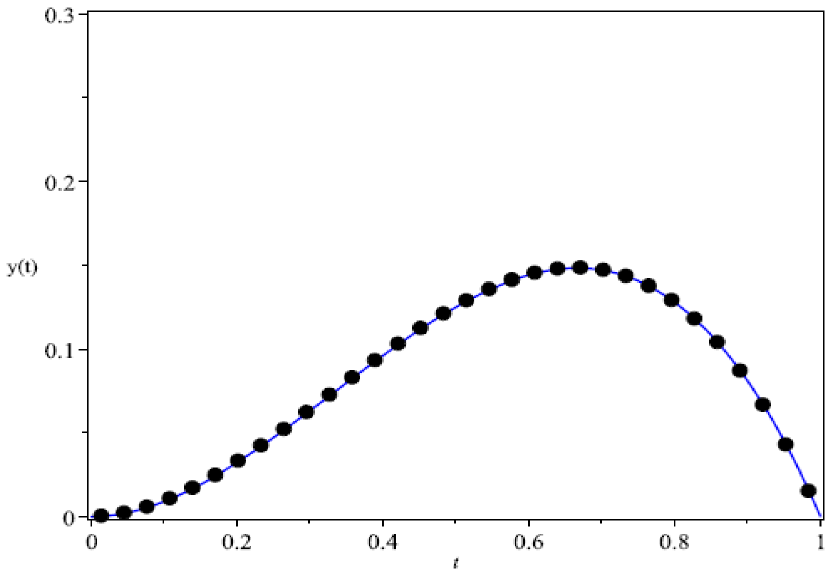

Fig. 3. Numerical (solid circle) and analytic (solid line) graph of solution of Example. 2, for K=32.

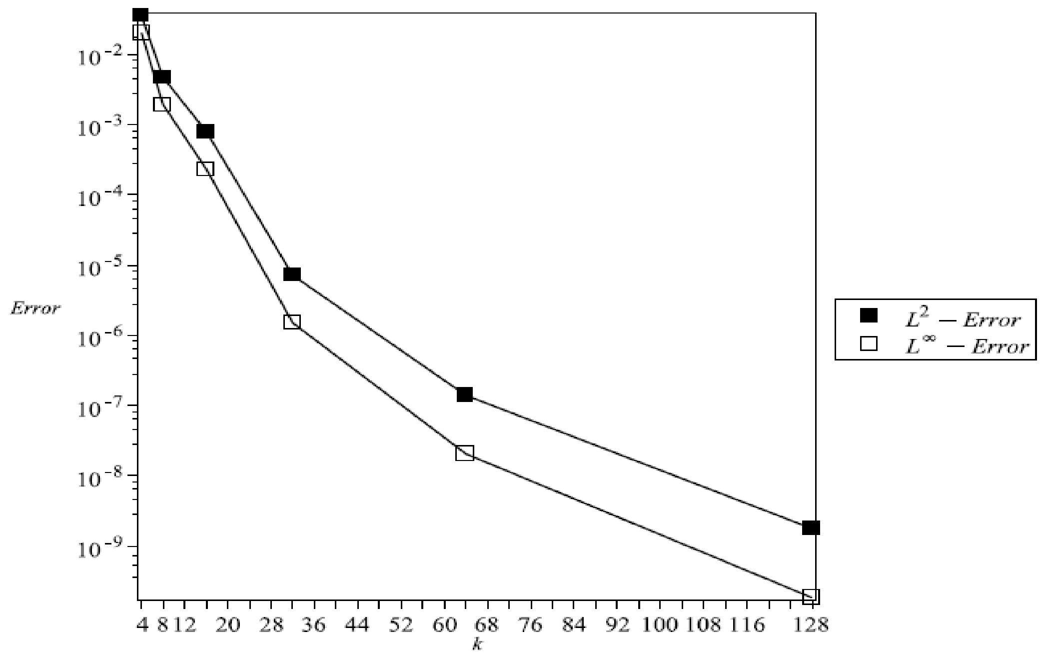

Fig. 4. Plot of the logarithmic scale of L^2 and L^∞- Error versus k, for Example 2.

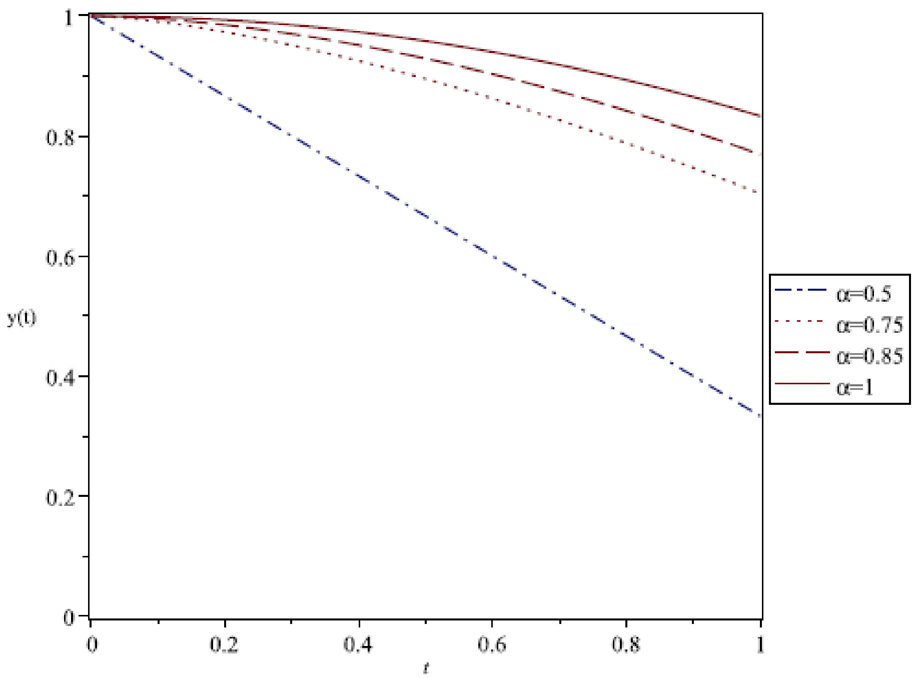

Fig. 5. Approximation of the solution for different values of α for $k = 64$ for Example 3.

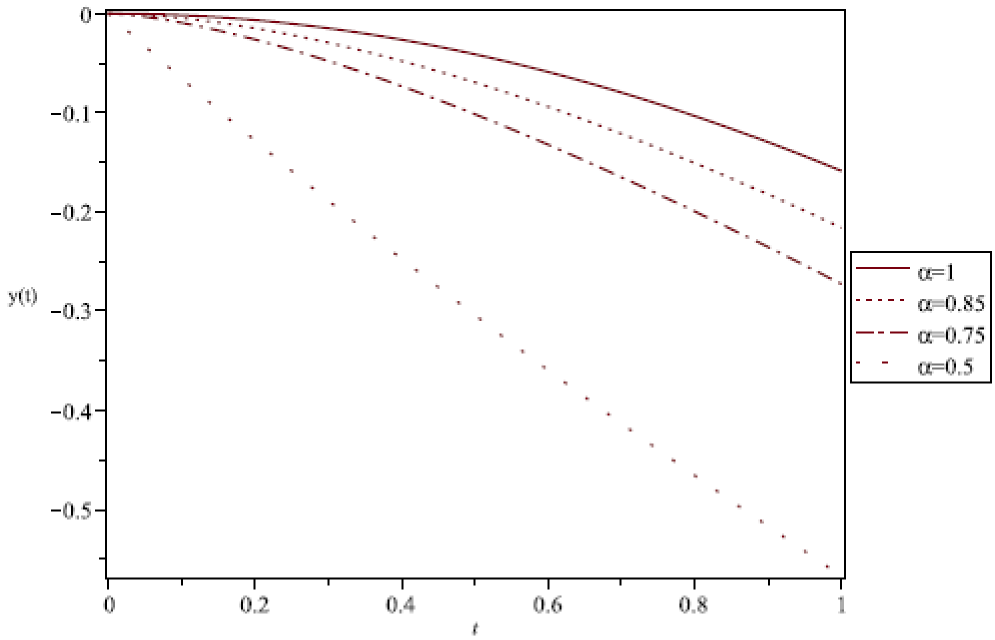

Fig. 6. Approximation of the solution for different values of α for k = 64 for Example 4.

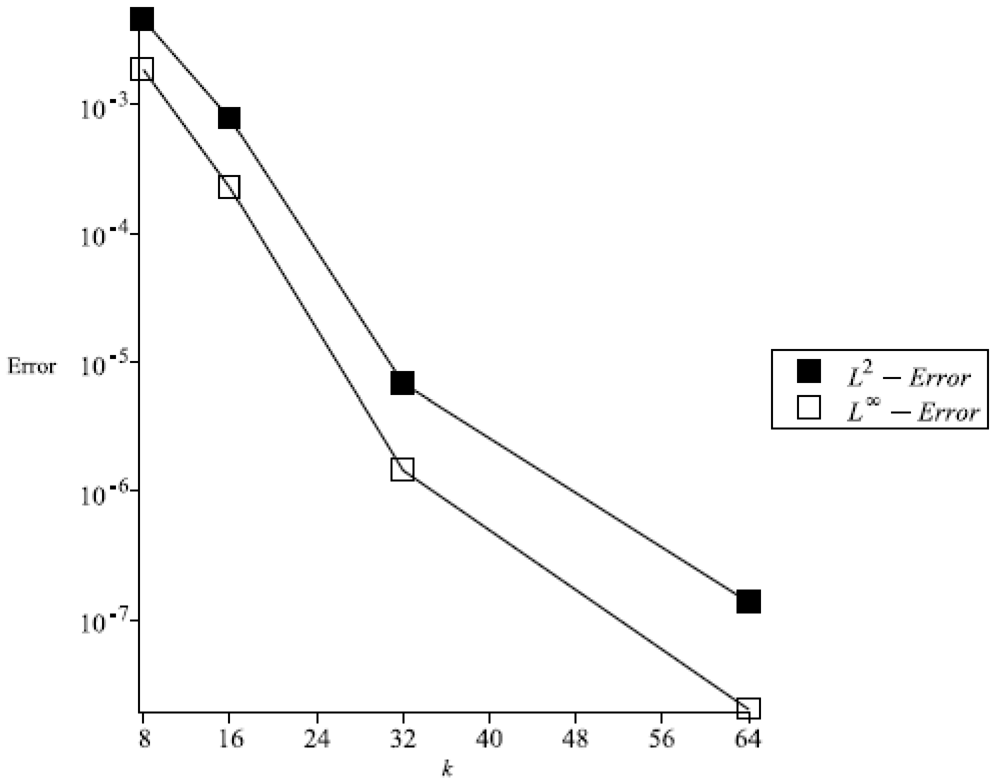

Fig. 7. Plot of the logarithmic scale of L^2 and L^∞- Error versus k, for for Example 4.

References

[1] A. Pirkhedri and H. H. S. Javadi, "Solving the time-fractional diffusion equation via sinc–haar collocation method," Applied Mathematics and Computation, pp. 317–325, 2015.

[2] J. Lane, "On the theoretical temperature of the sun under the hypothesis of a gaseous mass maintaining its volume by its internal heat and depending on the laws of gases known to terrestrial experiment," The American Journal of Science and Arts, vol. 50, pp. 57–74, 1870.

[3] R. Emden, Gaskugeln, Teubner. Leipzig and Berlin, 1907.

[4] K. Parand and A. Pirkhedri, "Sinc-collocation method for solving astrophysics equations," New. Astr., vol. 15, pp. 533–537, 2010.

[5] R. Saadeh, A. Burqan, and A. El-Ajou, "Reliable solutions to fractional laneemden equations via laplace transform and residual error function," Alexandria Engineering Journal, vol. 61, pp. 10551–10562, 2022.

[6] A. Akg¨ul, M. Inc, E. Karatas, and D. Baleanu, "Numerical solutions of fractional

differential equations of lane-emden type by an accurate technique," Advances in Difference Equations, pp. 220–232, 2015.

[7] M. Mechee and N. Senu, "Numerical study of fractional differential equations of lane-emden type by method of collocation," Applied Mathematics, vol. 3, pp. 851–856, 2012.

[8] G. Manish, P. Amit, and B. Dumitru, "An efficient hybrid computational technique for the time-dependent lane-emden equation of arbitrary order," Journal of Ocean Engineering and Science, vol. 7, no. 2, pp. 131–142, 2022.

[9] S. Liao, "On the homotopy analysis method for nonlinear problems," Appl. Math. Comput., vol. 147, no. 2, pp. 499–513, 2004.

[10] H. Marasi, N. Sharifi, and P. Hossein, "Modified differential transform method for singular lane-emden equations in integer and fractional order," TWMS J. Appl. Eng. Math., vol. 5, no. 1, pp. 124–131, 2015.

[11] A. Nasab, Z. Atabakan, A. Ismail, and R. Ibrahim, "A numerical method for solving singular fractional lane–emden type equations," Journal of King Saud University-Science, vol. 30, no. 1, pp. 120–130, 2018.

[12] A. K. Dizicheh, S. Salahshour, A. Ahmadian, and D. Baleanu, "A novel algorithm based on the legendre wavelets spectral technique for solving the lane–emden equations," Applied Numerical Mathematics, vol. 153, no. 1, pp. 443–556, 2020.

[13] J. Jaiswal and K. Yadav, "Method for solving lane–emden type differential equations by coupling of wavelets and laplace transform," Int. J. Adv. Math, vol. 153, no. 1, pp. 15–26, 2019.

[14] M. Abdelhakem and Y. Youssri, "Two spectral legendre's derivative algorithms for lane-emden, bratu equations, and singular perturbed problems," Applied Numerical Mathematics, pp. 243–255, 2021.

[15] M. Izadi, "A discontinuous finite element approximation to singular lane-emden type equations," Applied Numerical Mathematics, vol. 401, p. 126115, 2021.

[16] W. Abd-Elhameed, E. Doha, A. Saad, and M. Bassuony, "New galerkin operational matrices for solving lane-emden type equations," Applied Numerical Mathematics, vol. 52, pp. 83–92, 2016.

[17] M. Erfanian and A. Mansoori, "Solving the nonlinear integro-differential equation in complex plane with rationalized haar wavelet," Mathematics and Computers in Simulation, vol. 165, pp. 223–237, 2019.

[18] M. Razzaghi and Y. Ordokhan, "Solution of differential equations via rationalized haar functions," Math. Comput. Simul., vol. 56, pp. 235–246, 2001.

[19] Y. Li and W. Zhao, "Haar wavelet operational matrix of fractional order integration and its applications in solving the fractional order differential equations," Applied Numerical Mathematics, vol. 216, p. 2276–2285, 2010.

[20] C. Chen, M. Yi, and C. Yu, "Error analysis for numerical solution of fractional differential equation by haar wavelets method," J. Comput. Sci., vol. 3, p. 367–373, 2012.

[21] A. M. Malik, M. Yi, and O. H. Mohammed, "Two efficient methods for solving fractional lane–emden equations with conformable fractional derivative," Journal of the Egyptian Mathematical Society, vol. 28, pp. 42–53, 2020